Identification of an Active Site Ligand for a Group I Ribozyme Catalytic Metal Ion†

Alexander A. Szewczak,‡,§ Anne B. Kosek,‡ Joseph A. Piccirilli,|| and Scott A. Strobel*,‡

Department of Molecular Biophysics and Biochemistry and Department of Chemistry, Yale University, 260 Whitney Avenue, New Haven, Connecticut 06520-8114, and Howard Hughes Medical Institute, Department of Biochemistry and Molecular Biology and Department of Chemistry, The University of Chicago, 5841 South Maryland Avenue, MC1028, Chicago, Illinois 60637

Received October 25, 2001; Revised Manuscript Received December 26, 2001

ABSTRACT: The transition state of the group I intron self-splicing reaction is stabilized by three metal ions. The functional groups within the intron substrates (guanosine and an oligoribonucleotide mimic of the 5′-exon) that coordinate these metal ions have been systematically defined through a series of metal ion specificity switch experiments. In contrast, the catalytic metal ligands within the ribozyme active site are unknown. In an effort to identify them, stereospecific (R_P or S_P) single-site phosphorothioate substitutions were introduced at five phosphates predicted to be in the vicinity of the catalytic center (A207, C208, A304, U305, and A306) within the *Tetrahymena* intron. Of the 10 ribozymes that were studied, four phosphorothioate substitutions (A207 S_P, C208 S_P, A306 R_P, and A306 S_P) exhibited a significant reduction in the cleavage rate. Only the effect of the C208 S_P phosphorothioate substitution could be significantly rescued by the addition of a thiophilic metal ion, either Mn^{2+} or Zn^{2+}, when tested with an all-oxy substrate. The effect was not rescued with Cd^{2+}. To determine if one of the catalytic metal ions is coordinated to the C208 *pro*-S_P oxygen, the phosphorothioate-substituted ribozymes were also assayed using oligonucleotide substrates with a 3′-phosphorothiolate or an S_P phosphorothioate substitution at the scissile phosphate. This resulted in a second metal specificity switch, in that Mn^{2+} or Zn^{2+} no longer rescued the C208 S_P ribozyme, but Cd^{2+} provided efficient rescue in the context of either sulfur-containing substrate. The 3′-oxygen and the *pro*-S_P oxygen of the scissile phosphate are both known to coordinate the same metal ion, M_A, which stabilizes the negative charge on the leaving group 3′-oxygen in the transition state. Taken together, these data suggest that metal M_A is coordinated to the C208 *pro*-S_P phosphate oxygen, which constitutes the first functional link between a specific catalytic metal ion and a particular functional group within the group I ribozyme active site.

Ribonucleic acids (RNAs) can transmit genetic information, provide recognition elements for protein binding, form large macromolecular complexes, and directly or indirectly catalyze numerous chemical reactions in the cell (*1*). The recently determined crystal structures of the large and small ribosomal subunits have revealed a wide variety of RNA structural motifs and RNA−RNA and RNA−protein interactions (*2*, *3*), and provided a glimpse into the mechanism of peptide bond formation (*4*). However, the structures of many other RNAs remain unknown, and the catalytic mechanisms for RNAs are poorly understood in general.

To date, there is evidence that at least two basic catalytic strategies are employed by naturally occurring RNA enzymes: direct functional group participation and participation of bound divalent metal ions. In one strategy, proposed for the HDV ribozyme (*5*, *6*), the hairpin ribozyme (*7*, *8*), and the ribosome (*4*, *9*), RNA heterocyclic ring functional groups are predicted to participate directly in catalysis, perhaps by general acid−base or charge delocalization mechanisms. In the other strategy, Mg^{2+} ion cofactors bound by a ribozyme play roles in stabilizing the transition state. Divalent metal ions are particularly important for activity of the group I and group II introns, RNase P, and the spliceosome, where RNA phosphates and other functional groups have been proposed to coordinate magnesium ions in the proper positions to facilitate catalysis (*10*−*17*). However, high-resolution structural information about catalytic divalent metal ions within ribozyme active sites has remained elusive.

The *Tetrahymena* group I self-splicing intron is an example of an RNA enzyme that requires divalent metal ions for catalysis, as well as for stabilization of its tertiary structure (*18*). Thiophilic metal ion rescue of specific sulfur-substituted substrates has proven to be useful for defining the catalytic roles of specific metal ions coordinated to the splicing reaction substrates (*11*, *19*−*21*). Sulfur has much less affinity for Mg^{2+} than does oxygen (*22*). In such experiments, the substitution of sulfur for a phosphate oxygen inhibits binding of Mg^{2+} and disrupts ribozyme activity if the phosphate is involved in binding an important structural or catalytic metal. The ribozyme form of the *Tetrahymena* intron allows a

† This work was supported by NIH Grant GM54839 to S.A.S. J.A.P. is supported by the Howard Hughes Medical Institute.

* To whom correspondence should be addressed. Telephone: (203) 432-9772. Fax: (203) 432-5767. E-mail: strobel@csb.yale.edu.

‡ Yale University.

§ Present address: Department of Research Technologies, Bayer Pharmaceutical Corp., 400 Morgan Lane, West Haven, CT 06516.

|| The University of Chicago.

10.1021/bi011973u CCC: $22.00
Published on Web 02/01/2002

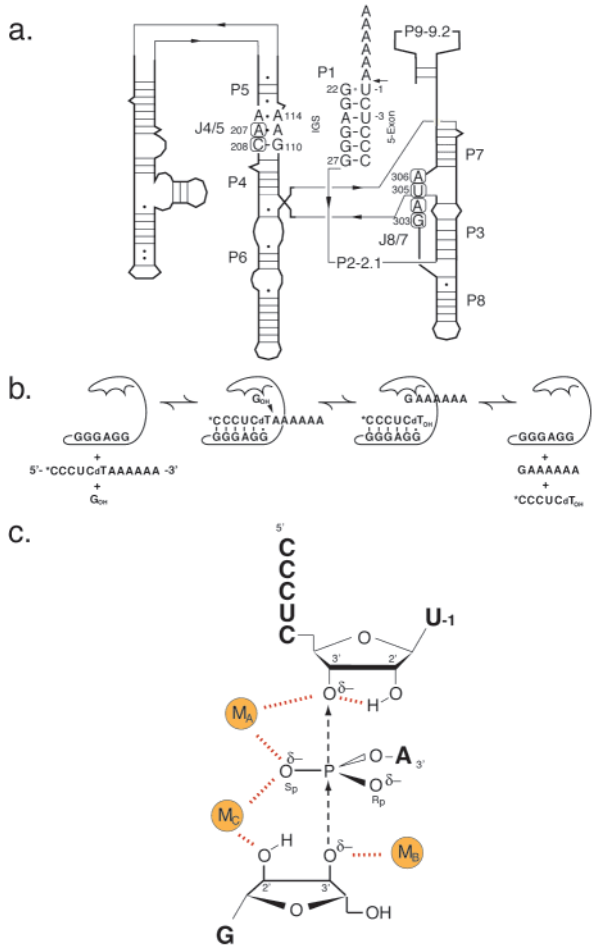

FIGURE 1: Secondary structure and cleavage reaction of the *Tetrahymena* ribozyme. (a) Schematic secondary structure of the *Tetrahymena* intron, with a bound substrate oligonucleotide that mimics the 5′-exon. Important elements of secondary sequence (P1, J8/7, J4/5, and P7) and the locations of nucleotides discussed in the text are marked. Boxes mark the six residues in J4/5 and J8/7 that are closest to the 3′-oxygen leaving group in the substrate (*32*). Thick lines show the schematic secondary structure of the intron, and thin lines with arrows illustrate the connectivity between sequence elements. Labels P and J denote paired helical elements and joining regions between helices, respectively (*50*). The P2-2.1 and P9 extension secondary structures have been omitted for clarity, but are included in the RNA constructs that were studied. (b) Oligonucleotide cleavage reaction catalyzed by the *Tetrahymena* ribozyme. The ribozyme binds exogenous guanosine in the P7 guanosine binding site and an oligonucleotide substrate that pairs with the internal guide sequence (IGS). The substrate−internal guide sequence helix is docked via stabilizing tertiary interactions into the core of the ribozyme, and the bound guanosine is positioned so that its 3′-OH group attacks the scissile phosphate and cleaves the oligo substrate, in the process becoming covalently attached to the 3′-half of the substrate. This form of the ribozyme is also used to bind a product oligonucleotide to measure substrate affinity (*42*). (c) Two-dimensional scheme for the transition state in which the incoming guanosine is in the process of displacing the 5′-portion of the substrate oligonucleotide. Divalent metals are shown in gold balls, and dashed lines show the network of interactions that stabilize the nucleophile and leaving group. Evidence suggests the presence of three divalent metal ions (M_A, M_B, and M_C) which interact with the substrate during cleavage (*19*−*21*, *23*, *24*), but the location of these metals within the ribozyme is a matter of investigation.

simplified version of the first step of splicing to be studied as a cleavage reaction using a short oligonucleotide and guanosine as substrates (see Figure 1b).

Three metal ions act to stabilize the group I intron transesterification reaction. Thiophilic metal ion rescue of a 3′-thiolate-substituted oligonucleotide demonstrated that a Mg^{2+} ion interacts with the 3′-oxygen leaving group in the ribozyme cleavage reaction (Figure 1c, M_A) (*19*). Similar experiments with a sulfur-substituted dinucleotide using an assay that mimics the reverse of the first step of splicing showed that a different Mg^{2+} metal (Figure 1c, M_B) interacts with the incoming 3′-oxygen on the guanosine nucleophile (*21*). Subsequent metal ion rescue experiments also identified a third metal (Figure 1c, M_C), one that interacts with the 2′-hydroxyl group on the guanosine (*23*, *24*). Recently, double sulfur metal ion specificity switch experiments have linked the *pro*-S_P oxygen on the substrate and the 3′-leaving group oxygen to the same metal (Figure 1c, M_A) (*20*, *25*). Furthermore, the metal M_C has been linked to both the *pro*-S_P substrate oxygen and the 2′-OH on the incoming guanosine (*25*). Thus, four different ligands in the substrate molecules have been experimentally linked to three different catalytic metals.

While this provides a fairly clear view of how metal cations contribute to RNA catalysis, none of these metals have been localized within the greater context of the ribozyme active site. Several clues are available, however. Approximately 40 individual *pro*-R_P phosphate oxygens scattered throughout the intron contribute to ribozyme activity. These were initially identified by nucleoside phosphorothioate interference experiments using RNA transcripts synthesized by T7 RNA polymerase in the presence of low levels of α-thionucleoside triphosphates (*26*). Subsequent thiophilic (Mn^{2+}) metal ion rescue experiments provided data that at the time were interpreted as evidence for direct coordination by magnesium ions at several positions in the core of the *Tetrahymena* intron (*27*). However, such approaches do not distinguish between a structural or a catalytic role for a metal ion, nor is it clear that they uniquely distinguish between inner sphere and outer sphere coordination (*28*). Furthermore, because T7 RNA polymerase will only use the S_P NTP isomer as a substrate (inverting the configuration to R_P upon incorporation), only half of the phosphate oxygens in an RNA molecule can be assayed.

A model of the intron active site has been generated using nucleotide analogue interference mapping (NAIM)[1] (*29*) and nucleotide analogue interference suppression (NAIS) data as distance constraints (*30*−*33*). The data indicate that the ribozyme specifically recognizes the phylogenetically conserved G·U wobble pair at the 5′-splice site (the P1 substrate helix) via interactions with a G·U wobble receptor in the conserved J4/5 region. The ribozyme also binds the P1 substrate helix through an extended minor groove triplex with the J8/7 region. The 5′-end of J8/7 is buttressed against the inside of the ribozyme core by a Hoogsteen base triple with the P3 helix. Thus, the structure appears to be highly interdependent and contains several layers of stabilizing hydrogen bonds.

Given the coordination constraints of the active site metals relative to the substrates, this model predicts that the phosphate oxygens of nucleotides in J8/7, J4/5, and/or the

[1] Abbreviations: NAIM, nucleotide analogue interference mapping; PAGE, polyacrylamide gel electrophoresis; PCR, polymerase chain reaction.

2′-hydroxyl of a residue in J8/7 may serve as ligands for the catalytic metal ion that stabilizes the 3′-oxygen leaving group at residue U(−1) (Figure 1c, M_A) (*19*, *32*). On the basis of this model, potential ligands that are in the proximity of the U(−1) 3′-oxygen are the *pro-*R_P and *pro-*S_P oxygens of A207 and C208 in J4/5 and A304 and U305 in J8/7 (see Figure 1a). We report here the results of single and double sulfur atomic substitution experiments that tested whether these groups are involved in binding catalytic metal ions. These experiments identify the first ligand for a catalytic divalent metal ion within the group I intron active site.

MATERIALS AND METHODS

RNA Constructs and Oligonucleotides. Semisynthetic ribozymes with specific sulfur substitutions were created by covalently joining three component pieces of the *Tetrahymena* ribozyme. Plasmids used for RNA component transcription included pUCP1-P5SunY, pUCP4-P9, pUCL-21G414, pUCmP1-P8SunY, and pUCP9. Plasmids pUCP4-P9 and pUCL-21G414 were generated as described previously (*30*, *34*). Plasmid pUCP9 was created by PCR amplification of pUCL-21G414. Plasmid pUCmP1-P8SunY was created by separate PCR amplification of plasmids pUCP1-P5SunY (primers mP1P8sun2 and suny3′) and pUCL-G414 (primers UP1212 and mP1P8sun1). The products of the two reactions were then pooled and PCR amplified again using primers UP1212 and suny3′. The resulting *Eco*RI−*Hin*dIII fragment containing the fused P1-P8 and SunY sequences was subcloned into pUC19. The primers used for PCR had the following sequences: mP1P8sun2, 5′-d(ATTAACGTAAGTCAAGTGCGAGTAAAATCTGCCTAAACG)-3′; suny3′, 5′-d(ATTAAGCTTCTCTTCAGATCCTGCATGTCACC)-3′; mP1P8sun1, 5′-d(ACTTGACTTACGTTAATGCGACCAATGCATAATCACCGACCGACATTT)-3′; and UP1212, 5′-d(GTTTTCCCAGTCACGAC)-3′. The DNA splint used for RNA ligation was mJ8/7, with the sequence 5′-d(CCATTAAGGAGAGGTCCGACTATATCTTATGCGACCAATACAT)-3′. Plasmid DNA sequences were confirmed by dideoxy sequencing. DNA oligonucleotides were obtained from the HHMI Biopolymer & W. M. Keck Biotechnology Resource Laboratory at Yale University.

Plasmid pUCP9 contains the coding sequence for nucleotides 313−410 of the *Tetrahymena* group I intron sequence downstream of a T7 RNA polymerase promoter. Digestion of pUCP9 with the restriction endonuclease *Sca*I produces a template for runoff transcription. Plasmid pUCmP1-P8SunY contains the coding sequence for *Tetrahymena* nucleotides 22−300, downstream of a T7 promoter. The plasmid also contains mutations that convert Watson−Crick pairs to wobble pairs within the P8 helix (hence, m for mutant, "mP1-P8"). These mutations improve ligation efficiency by destabilizing the P8 secondary structure while stabilizing binding of the complementary mJ8/7 DNA splint. Mutation or extension of this helix does not interfere with ribozyme activity (*35*). In addition, the small SunY self-splicing group I intron (*36*) was placed downstream of the *Tetrahymena* P1-P8 sequence to produce a homogeneous 3′-end at residue 300. Digestion with *Ear*I produces a template for runoff transcription of the fused intron sequences. During the transcription reaction, the SunY intron catalyzes its own cleavage from the full-length RNA, leaving the appropriate shorter *Tetrahymena* sequence with a 3′-terminal hydroxyl group suitable for ligation.

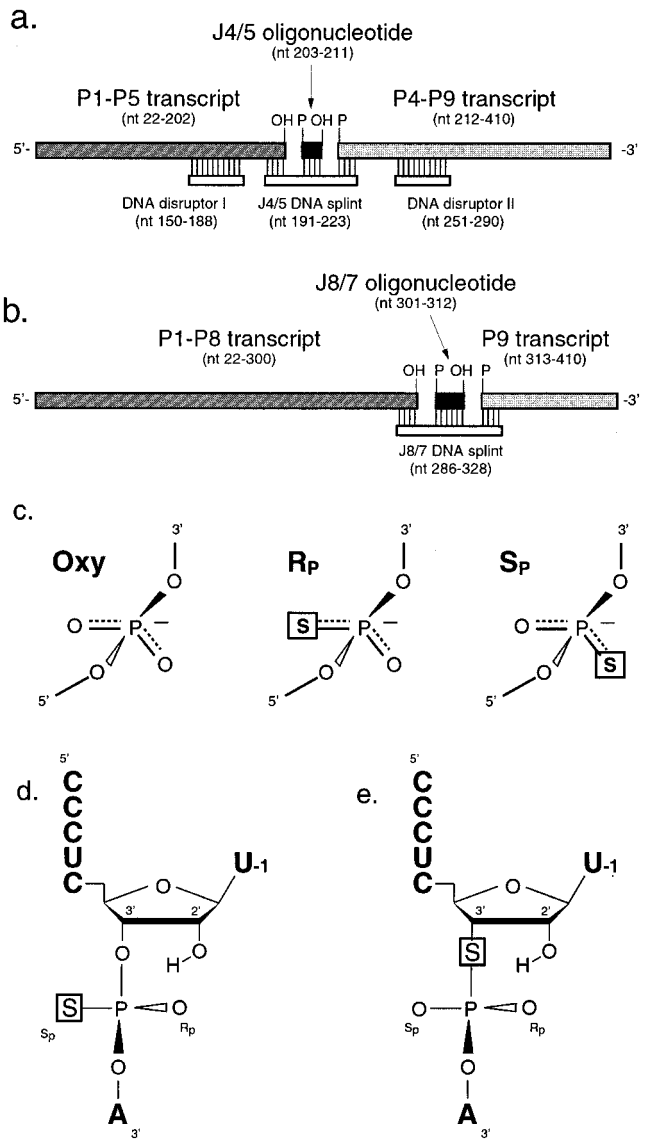

FIGURE 2: Ribozyme and substrate oligonucleotide sulfur substitutions. (a) Three-piece ligation scheme for preparing ribozymes with phosphorothioate substitutions in J4/5. The J4/5 synthetic oligonucleotide (black) was ligated between P1-P5 (dark gray) and P4-P9 (gray) RNAs. In addition to the DNA splint, two other DNA oligonucleotides (disrupters I and II) were used to help unfold tertiary structures that interfere with ligation by T4 DNA ligase (*34*). (b) Three-piece J8/7 ligation scheme for constructing ribozymes with sulfur substitutions in J8/7. P1-P8, J8/7, and P9 RNA fragments are ligated together using a single DNA splint. (c) R_P and S_P ribozyme phosphorothioate backbone atomic substitutions (introduced at positions A207, C208, A304, U305, and A306). A box marks each site where a phosphate oxygen has been replaced with a sulfur. (d) S_P phosphorothioate-containing substrate oligonucleotide. (e) The 3′-phosphorothiolate-containing substrate oligonucleotide.

The all-oxygen and phosphorothioate-containing synthetic 2′-ACE RNA oligonucleotides r9 and r12 (corresponding to *Tetrahymena* nucleotides 203−211 and 301−312, respectively; see Figure 2), along with substrate and product oligonucleotides [P, 5′-CCCUCU-3′; rS, 5′-CCCUCUAAAAA-3′; dT(−1)S, 5′-CCCUCdTAAAAA-3′; $mCU_{S_p}A$, S_P diastereomer of 5′-C2′omeC2′omeC2′omeUCUP═SA-3′, $mCU_{R_p}A$, R_P diastereomer of 5′-C2′omeC2′omeC2′omeUCUP═SA-3′;

and mCUA, 5′-C2′omeC2′omeC2′omeUCUA-3′], were obtained from Dharmacon Research, Inc. (*37*). Substrate oligonucleotide dU3′sA (5′-C2′omeC2′omeC2′omeUCdU3′sA-3′) was synthesized as described previously (*20*). The 2′-*O*-methyl substitutions prevent miscleavage of the substrate at positions other than the scissile phosphate. This is necessary for experiments using the S_P phosphorothioate and thiolate substitutions because the rates of cleavage at the scissile phosphate are severely reduced. Synthetic oligonucleotides containing a phosphorothioate substitution were separated into S_P and R_P diastereomers by C18 reverse phase HPLC using a 0 to 20% gradient of a B/A mixture (solvent A, 0.1 M NH_4OAc; solvent B, 20% A and 80% CH_3CN). The R_P and S_P isomers were well-resolved, with the R_P isomer eluting from the column first. Purified fractions were dried, redissolved in 10 mM Tris-HCl (pH 7.5) and 0.1 mM EDTA, and stored at −20 °C. The identity of each r12 diastereomer was confirmed by digestion with snake venom phosphodiesterase, which preferentially cleaves an R_P over an S_P phosphorothioate (*38*). The identity of the r9 diastereomers was confirmed by cleavage with *Tetrahymena* ribozymes with an internal guide sequence that had been mutated to bind the r9 oligonucleotide. The *Tetrahymena* ribozyme preferentially cleaves the R_P phosphorothioate substrate (*39*), and hence differentiates between the R_P and S_P diastereomers (data not shown). The purified r9 oligonucleotides were treated with T4 polynucleotide kinase (New England Biolabs) to add a phosphate to their 5′-ends prior to ligation (5 nmol of oligo, 100 nmol of ATP, 50 units of PNK, and 1× PNK buffer, at 37 °C for 1 h, in a final volume of 100 μL). Ribonucleotide substrates containing 3′-phosphorothiolate substitution were prepared as described previously (*40*).

Preparation of Ligated Ribozymes. Full-length *Tetrahymena* ribozymes with site specific and stereospecific phosphorothioate substitutions at nucleotides in J8/7 or J4/5 were prepared by RNA ligation using T4 DNA ligase (*41*). In the three-part ligation scheme employed here (see panels a and b of Figure 2), an internal short synthetic oligonucleotide was ligated to two longer flanking RNAs made by T7 RNA polymerase transcription, using DNA splints to align the RNA pieces. Ribozymes with sulfur substitutions at A207 or C208 in the J4/5 region were prepared by this general method using the P1-P5 and P4-P9 RNA constructs and oligonucleotide r9 as described previously (Figure 2a) (*34*).

Synthesis of ribozymes with atomic substitutions in the J8/7 region (A304, U305, or A306) was accomplished by a three-piece ligation (Figure 2b). The 5′-RNA transcript, P1-P8 (nucleotides 22−300), was synthesized using the plasmid pUCmP1-P8SunY digested with *Ear*I restriction endonuclease as a template for runoff transcription. The SunY cleavage product corresponding to P1-P8 RNA was isolated from the uncleaved precursor and the SunY ribozyme by PAGE. The 3′-RNA transcript, P9 (nucleotides 313−410), was transcribed using pUCP9 digested with *Sca*I restriction endonuclease. Transcription conditions for both RNAs were as follows: 75 μg/mL digested plasmid DNA, 40 mM Tris-HCl (pH 7.5), 10 mM DTT, 4 mM spermidine, 0.05% (v/v) Triton X-100, 1 unit/mL inorganic pyrophosphatase (Sigma-Aldrich), and 80 μg/mL T7 RNA polymerase. Reaction mixtures were incubated at 37 °C for 2 h. For the 3′-RNA transcript, an excess of GMP (20 mM) was added to the P9 RNA transcription reaction to ensure that the RNA had a single phosphate compatible with ligation on the 5′-end. For the P9 transcriptions, 15 mM $MgCl_2$ and NTPs (2 mM each) were used; the P1−P8 transcriptions contained 40 mM $MgCl_2$ and NTPs (4 mM each). The increased $MgCl_2$ concentration helped to improve the efficiency of 3′-end processing by SunY. Transcribed RNAs were purified by PAGE (6%, 7 M urea). Bands were visualized by UV shadowing and cut out of the gel. RNAs were eluted overnight at 4 °C into 10 mM Tris-HCl (pH 7.5), 0.1 mM EDTA, and 250 mM NaCl, then precipitated with 3 volumes of ethanol, and stored at −20 °C. Typical final yields of purified RNA were approximately 3−6 nmol/mL of transcription reaction mixture.

J8/7 ligation reaction conditions were similar to those described previously for the J4/5 constructs (*34*), except that yields were improved significantly by using as small a reaction volume as possible and by further optimizing buffer conditions and the temperature of ligation. Unlike the J4/5 ligations, the J8/7 constructs did not need added DNA disruptors to help melt out RNA tertiary structure. For each ligation reaction, 1 nmol of mP1-P8, 2 nmol of P9, 2 nmol of mJ8/7 splint DNA, and 2 nmol of phosphorylated r12 were mixed together in a minimum volume (typically, ≤100 μL) of 25 mM Tris-HCl (pH 7.5) and 25 mM NaCl. The RNAs and DNAs were annealed by heating to 90 °C for 5 min, and then slowly cooling to room temperature. The buffer was adjusted to final concentrations of 50 mM Tris-HCl (pH 7.5), 10 mM $MgCl_2$, 10 mM DTT, 1 mM ATP, 25 μg/mL BSA, and 500 units of T4 DNA ligase. The reaction mixture was incubated for 4 h at 37 °C, and the full-length RNAs were separated from the partial ligation products by PAGE (6%, 7 M urea). The bands corresponding to the full-length ribozyme were excised from the gel, eluted overnight at 4 °C into 10 mM Tris-HCl (pH 7.5), 0.1 mM EDTA, and 250 mM NaCl, and then ethanol precipitated. Ribozymes were redissolved into 10 mM Tris-HCl (pH 7.5) and 0.1 mM EDTA and stored at −20 °C.

Substrate Binding Affinity Measurements. Substrate−ribozyme binding affinity was measured using a product oligonucleotide gel shift assay (*33*, *42*). The ribozyme mix was prepared by dissolving various amounts of ribozyme into binding buffer [50 mM Tris-HCl (pH 7.5), 0.1 mM EDTA, 100 mM NaCl, and 4 mM $MgCl_2$]. The ribozyme mix was heated at 50 °C for 10 min and then cooled to 40 °C to ensure proper folding of the ribozyme (*43*). The substrate mix contained 8 pM 5′-^{32}P-labeled 5′-CCCUCU-3′ in binding buffer with 20% glycerol and 0.04% xylene cyanol. This solution was preheated to 40 °C. To initiate binding, equal volumes of the ribozyme mix (2× final ribozyme concentration and 1× buffer) and the substrate mix (2× final substrate concentration and 1× buffer with 2× glycerol and 2× loading dye) were added together, and heated at 40 °C for 10 min. The RNA complexes were analyzed by 10% native PAGE [34 mM Tris-HCl (pH 7.5), 66 mM HEPES, 0.1 mM EDTA, and 4 mM $MgCl_2$]. Experiments were performed with ribozyme at concentrations ranging from 1 pM to 200 nM. Calculated values for the binding constant were obtained by plotting the fraction of bound oligonucleotide as a function of ribozyme concentration using Kaleidagraph (Synergy Software), and fitting the data to eq 1:

$$\text{fraction bound} = B[\text{R}]/([\text{R}] + K_{\text{D}}) \quad (1)$$

where [R] is the ribozyme concentration, K_D is the dissociation constant, and B is the fraction of substrate competent to bind to the ribozyme (typically, ~90%).

Ribozyme Kinetics. Ribozyme kinetics were measured using a substrate oligonucleotide cleavage assay. Single-turnover cleavage reactions were performed using saturating final concentrations of ribozyme (typically, between 50 and 200 nM), 1 mM GMP, 2 nM 5′-^{32}P-labeled RNA oligonucleotide substrate, 4 or 10 mM $MgCl_2$, and either 50 mM MES (pH 5.5) or 50 mM HEPES (pH 7.0). To initiate the reaction, 10 μL each of a ribozyme mix (2× ribozyme and 1× buffer) and a substrate mix (2× substrate, 2× GMP, and 1× buffer) were heated at 50 °C for 10 min, mixed, and further incubated at 50 °C. At various times, 2 μL aliquots were removed from the reaction mixture and the reactions quenched with 4 μL of loading buffer (95% formamide, 25 mM EDTA, 0.025% xylene cyanol, and 0.025% bromophenol blue). Reaction products were analyzed by denaturing PAGE (15%, 7 M urea). The fraction of uncut substrate oligonucleotide was plotted as a function of time, and kinetic rate constants were calculated by fitting the data to eq 2 using Kaleidagraph (Synergy Software):

$$\text{fraction uncut} = (1 - \text{NR}) \times \exp(-kt) + \text{NR} \quad (2)$$

where t is time, NR is the nonreactive fraction of substrate (typically, 5%), and k is the first-order rate constant. Each rate curve was fit using a minimum of seven data points.

For the thiophilic metal rescue experiments, the total divalent metal ion concentration was held constant at 10 mM and the appropriate amount of thiophilic metal ion added to the reaction buffers. DTT (10 mM) was added to the gels and running buffer used for PAGE analysis of reaction products derived from the thiolate-containing substrate oligonucleotide (*19*). Thiophilic metal stock solutions were as follows: 100 mM $Mn(OAc)_2$ in H_2O, 100 mM $CdCl_2$ in 50 mM MES (pH 6.0), and 100 mM $ZnCl_2$ in 50 mM MES (pH 6.0).

The addition of Mn^{2+} in and of itself increases the rate of the *Tetrahymena* ribozyme when compared to the rate of the reaction in Mg^{2+}. To control for this and any other nonspecific rate enhancements caused by the added divalent metals, kinetic rates measured with sulfur-containing substrates were normalized to the rate of the reaction with an all-oxygen substrate in the presence of the same metal. Similarly, sulfur-substituted ribozyme rates were normalized to an all-oxygen ribozyme control performed with the same thiophilic metal. The magnitudes of the fully normalized thiophilic metal ion rescue effects were therefore calculated using eq 3:

$$(K_{\text{rel}} \text{ with S-ribozyme, S-substrate, } M^{2+}/K_{\text{rel}} \text{ with S-ribozyme, S-substrate, } Mg^{2+})/(K_{\text{rel}} \text{ with S-ribozyme, O-substrate, } M^{2+}/K_{\text{rel}} \text{ with S-ribozyme, O-substrate, } Mg^{2+}) \quad (3)$$

where each K_{rel} is the rate of a sulfur-containing ribozyme normalized to the all-oxygen wild-type ribozyme under the same reaction conditions and with the same substrate. Each full double sulfur rescue effect is therefore calculated using eight measured rates.

RESULTS

Within the overall architecture of the *Tetrahymena* ribozyme model constructed using NAIM and NAIS data (*32*, *33*), the J4/5 and J8/7 secondary structure elements come together to form part of the molecule's active site (see Figure 1). Nine functional groups in these two regions are positioned such that they might participate in coordinating the metal ion that stabilizes the 3′-oxygen leaving group in the *Tetrahymena* cleavage reaction. These are the phosphate oxygens of A207 and C208 in J4/5, the phosphate oxygens of A304 and U305 in J8/7, and the 2′-OH group of G303 (also in J8/7) (*32*). To test which, if any, of these atoms might participate in binding catalytic metals, we created semisynthetic ribozymes with atomic substitutions at these positions, and at one other nearby location, the phosphate of A306 in the P7 helix. We replaced the phosphate oxygens with sulfur because Mg^{2+}, a hard Lewis acid, has a lower affinity for sulfur than softer Lewis acids (*22*). We also replaced the 2′-OH at residue G303 with a 2′-H, which did reduce the binding affinity and kinetic activity of the ribozyme 13- and 18-fold, respectively, but this substitution was not characterized further. Synthetic oligonucleotides were obtained as a racemic mixture of both the R_P and S_P configurations. By separating the diastereomers (see Materials and Methods), we could create diastereomerically pure ribozymes with a single R_P or S_P sulfur substitution. We prepared a total of 10 sulfur-substituted ribozymes, and two "wild-type" all-oxygen-containing ligated ribozymes as controls: A207 R_P and S_P, C208 R_P and S_P, A304 R_P and S_P, U305 R_P and S_P, A306 R_P and S_P, and Wt r9 and Wt r12 (see Figures 1 and 2). To incorporate the sulfur substitutions, we employed the three-part ligation schemes illustrated in Figure 2. In this strategy, a short internal oligonucleotide is ligated by T4 DNA ligase between two longer T7 RNA polymerase transcripts. Yields were typically ~20% ligated full-length RNA.

Effects of Phosphorothioate Substitution on Oligonucleotide Binding. Because of the structural role that specific metal ions often play in stabilizing the *Tetrahymena* ribozyme, sulfur substitutions might reduce ribozyme activity merely by disrupting binding of the substrate oligonucleotide. To control for such binding effects, the affinity of each ribozyme for the product oligonucleotide 5′-CCCUCU-3′ was measured using a gel shift assay (see Figure 3a). As can be seen from Table 1, binding was affected for a subset of the substituted ribozymes. Replacing the *pro*-R_P oxygen of A207, the *pro*-R_P oxygen of A304, or the *pro*-R_P oxygen of A306 had little effect on substrate affinity. Replacing the *pro*-S_P phosphate oxygen with sulfur at A207 or substituting an S_P sulfur at U305 only decreased binding by ~2-fold. In contrast, five of the substitutions reduced binding affinity by 10−20-fold: C208 S_P, C208 R_P, A304 S_P, U305 R_P, and A306 S_P (see Table 1). Given the central location of these atomic groups within the ribozyme, it is perhaps not surprising that the majority of them affect binding to some extent. However, none of the effects are so dramatic as to suggest that the ribozyme tertiary structure is disrupted in a major way.

Effects of Phosphorothioate Substitution on the Cleavage Reaction. Taking the binding effects of each atomic substitu-

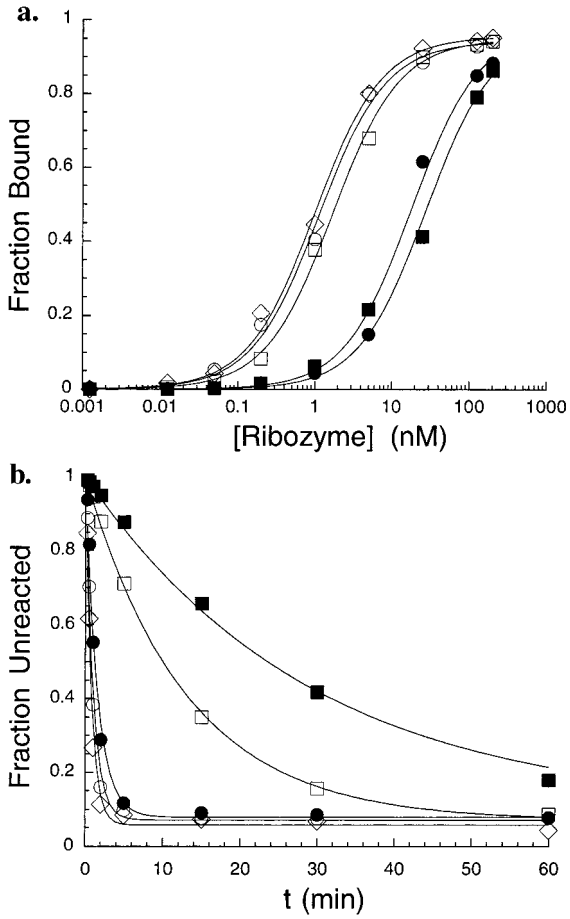

FIGURE 3: Binding affinity and kinetic rate measurements. (a) Gel shift assay for measuring the binding affinity of A207 and C208 phosphorothioate-substituted ribozymes for substrates. In each assay, the fraction of bound ^{32}P-labeled product oligonucleotide 5′CCCUCU-3′ is monitored as a function of ribozyme concentration over the range of 1.25 pM to 200 nM, and a semilog plot of fraction bound vs ribozyme concentration is fit to eq 1. (b) Cleavage assay for measuring ribozyme kinetic rates. The 5′-^{32}P-labeled substrate oligonucleotide 5′-CCCUCUAAAAA-3′ was reacted with wild-type and A207- or C208-substituted ribozymes, and the extent of cleavage was followed as a function of time. The fraction of unreacted substrate is plotted vs time, with the data fit to eq 2 to calculate the first-order kinetic rate constant: (◇) Wt r9, (○) A207 R_P, (□) A207 S_P, (●) C208 R_P, and (■) C208 S_P.

tion into account, we next performed single-turnover kinetic assays with 2 nM ^{32}P-labeled substrate oligonucleotide and saturating concentrations of each substituted ribozyme along with saturating GMP (see Figure 3b and Table 1). The activity of the ribozymes with single atomic substitutions falls into three main classes. One ribozyme, A304 R_P, showed no effect. Five ribozymes showed modest effects (2−5-fold), the five being A207 R_P, C208 R_P, A304 S_P, U305 R_P, and U305 S_P. However, four of the ribozymes showed substantially greater effects (25−50-fold), those being A207 S_P, C208 S_P, A306 R_P, and A306 S_P. This is in general agreement with the phosphorothioate interference data collected for the *pro*-R_P substitutions at these positions (*44*).

Metal Rescue of Phosphorothioate Effects. Soft metals such as Mn^{2+}, Zn^{2+}, and Cd^{2+} have much higher affinity for sulfur than Mg^{2+} (*22*) and can be used to identify a Mg^{2+} ion ligand by a sulfur substitution metal specificity switch (see, for example, ref *27*). To determine if any of the substitutions could be rescued by a thiophilic metal, we next

Table 1: *Tetrahymena* Ribozyme Sulfur Substitution Effects[a]

	binding affinity		cleavage rate		
	K_d (nM)[b]	rel.	[R] (nM)	k_{obs} (min^{-1})[c]	rel.
wild-type J4/5 9-mer	0.8 ± 0.2	1.0	50	1.55	1.00
A207 R_P	0.8 ± 0.3	1.0	50	0.78	0.50
A207 S_P	1.9 ± 0.3	2.5	50	**0.06**	**0.04**
C208 R_P	13 ± 5	16	100	0.59	0.38
C208 S_P	18 ± 9	24	100	**0.03**	**0.02**
wild-type J8/7 12-mer	1.8 ± 0.3	1.0	50	1.69	1.00
A304 R_P	1.1 ± 0.7	0.6	50	1.87	1.11
A304 S_P	22 ± 3	12	200	0.32	0.19
U305 R_P	23 ± 11	13	200	0.42	0.25
U305 S_P	3.4 ± 0.5	1.9	50	0.59	0.35
A306 R_P	1.2 ± 0.4	0.7	50	**0.06**	**0.04**
A306 S_P	33 ± 17	19	200	**0.06**	**0.04**

[a] Binding affinity measured with 5′-CCCUCU-3′; cleavage kinetics measured at pH 5.5 with 5′-CCCUCUAAAAA-3′. [b] Average of three independent measurements. The error is the standard deviation from the mean. [c] Average of two independent measurements for J4/5-substituted ribozymes.

Table 2: Thiophilic Metal Ion Rescue of Ribozyme Sulfur Substitutions[a]

	rate relative to that of the all-oxy ribozyme[b]				fold rescue		
	none	Mn^{2+}	Cd^{2+}	Zn^{2+}	Mn/Mg	Cd/Mg	Zn/Mg
A207 R_P	0.50	0.47	0.47	0.55	0.93	0.94	1.1
A207 S_P	0.04	0.08	0.18	0.22	1.9	4.4	5.2
C208 R_P	0.38	0.49	0.30	0.60	1.3	0.79	1.6
C208 S_P	0.02	0.30	0.04	0.39	**14**	1.8	**18**
A304 R_P	1.1	0.98	1.0	1.3	0.89	0.92	1.1
A304 S_P	0.19	0.28	0.27	0.07	1.5	1.4	0.38
U305 R_P	0.25	0.32	0.45	0.26	1.3	1.8	1.1
U305 S_P	0.35	1.0	0.33	0.64	2.9	0.94	1.8
A306 R_P	0.04	0.02	0.12	0.03	0.64	3.2	0.76
A306 S_P	0.04	0.04	0.09	0.05	1.1	2.5	1.2

[a] Rescue effect = (k_{obs} with S-ribozyme, metal/k_{obs} with O-ribozyme, metal)/(k_{obs} with S-ribozyme, no metal/k_{obs} with O-ribozyme, no metal). Rescue effect is >1.0 if the added thiophilic metal increases the rate of reaction relative to that of the all-oxygen wild-type ribozyme. [b] Metal concentrations: 1 mM Mn^{2+}, 0.5 mM Zn^{2+}, and 0.2 mM Cd^{2+}; total divalent cation concentration of 10 mM. Data collected with rS substrate at pH 5.5.

measured ribozyme cleavage rates of the ribo substrates in reaction buffers containing 9 mM $MgCl_2$ and 1 mM $Mn(OAc)_2$. The spectrum of Mn^{2+} rescue effects among the substituted ribozymes is shown in Table 2. All but one of the ribozyme substitutions that were tested were insensitive to the addition of Mn^{2+}. Of the four ribozymes that exhibited a substantial phosphorothioate effect, only C208 S_P was significantly affected by the addition of Mn^{2+}. The phosphorothioate effect was partially rescued (approximately 14-fold) in 1 mM Mn^{2+} compared to the 50-fold decrease in activity observed for C208 S_P substitution in the Mg^{2+}-only buffer. Thus, the C208 *pro*-S_P phosphate oxygen appears to be a primary candidate for Mg^{2+} ion coordination within the wild-type ribozyme. Thiophilic metal ion rescue experiments were also carried out with two other thiophilic metals, Cd^{2+} and Zn^{2+}. C208 S_P was partially rescued by Zn^{2+}, but not by Cd^{2+}. Neither metal showed any significant rescue of any of the other sulfur substitutions (see Table 2). It is important to note that the lack of rescue with Mn^{2+} or another thiophilic metal ion does not rule out the possibility of a particular oxygen coordinating a Mg^{2+} ion (*28*).

To identify ligands for the catalytic metal ions using metal ion rescue experiments, the kinetic assays must monitor the chemical step. We set out to confirm that chemistry is limiting for the C208 S_P ribozyme by measuring the rate of cleavage for a substrate with an R_P phosphorothioate substitution at the cleavage site ($mCU_{RP}A$) in comparison to the cleavage rate of an all-oxy-containing substrate (mCUA) under the same reaction conditions. For the wild-type ribozyme at low pH, the chemical step is limiting and the R_P sulfur substitution at the scissile phosphate results in a 2−3-fold phosphorothioate effect (*39*). The magnitude of the effect arises from the inherently less reactive nature of the R_P phosphorothioate. Consistent with chemistry being the rate-limiting step in the reaction, the C208 S_P ribozyme exhibited a 2.6-fold reduction in rate at 50 °C and pH 5.5 (0.023 min^{-1} for mCUA compared to 0.0087 min^{-1} for $mCU_{R_P}A$). This argues that the Mn^{2+} rescue of the C208 S_P ribozyme results from an increase in the chemical reaction rate.

Metal Specificity Switch of a Double Sulfur Substitution. Double sulfur substitution metal specificity switch experiments have been used to link the 3′-leaving group and *pro*-S_P phosphorothioate oxygens in the substrate to a single metal (*20*, *25*). In such experiments, adding a second sulfur to a metal binding site interferes with rescue by Mn^{2+}. However, differently sized thiophilic metals such as Cd^{2+} or Zn^{2+} ions have the potential to bind better to the double sulfur-substituted site. Observation of such a metal specificity switch provides evidence linking the two substituted functional groups to the same metal ion. We reasoned that similar experiments might allow us to link metal ligands in the substrate with C208 in the ribozyme itself, and thus locate a catalytic metal binding site in the ribozyme. Accordingly, we next performed kinetic assays with 5′-^{32}P-labeled sulfur-containing substrates and the J4/5-substituted ribozymes with phosphorothioates at A207 and C208. The 3′-S substrate, dU3′sA, contains a 3′-phosphorothiolate at the cleavage site, and the substrate $mCU_{S_P}A$ contains the S_P diastereomeric phosphorothioate at the cleavage site (see panels d and e of Figure 2). Both of these substrates change functional groups predicted to coordinate M_A, the metal stabilizing the leaving group (*25*). While addition of micromolar concentrations of Cd^{2+} can rescue the 3′-S modification (*19*, *20*), the S_P modification is only rescued at millimolar Cd^{2+} concentrations and at high Mg^{2+} concentrations (*25*).

When reactions were performed with the 3′-sulfur-substituted substrate and a J4/5 sulfur-substituted ribozyme, Mn^{2+} provided no significant improvement in activity with any of the four J4/5 sulfur-substituted ribozymes compared to that of the wild-type ribozyme (Table 3). Zn^{2+} did not rescue activity for any of the doubly substituted ribozymes, either. Of particular interest is that C208 S_P was inhibited 100-fold in the presence of Mn^{2+} when tested with the phosphorothiolate-substituted substrate. This is in sharp contrast to the 14-fold enhancement observed above with the unsubstituted substrate. Furthermore, significant rescue of activity (100-fold) exclusively for the C208 S_P ribozyme was observed upon addition of Cd^{2+} (see Table 3). Recall that Cd^{2+} had no positive effect on the rate of the C208 S_P ribozyme when tested with the all-oxy substrate. Furthermore, the calculated rescue effect normalizes for any nonspecific changes in activity due to the added thiophillic metal, or for rescue effects due solely to the presence of the sulfur in the substrate. This is done by including eight combinations of ribozyme, substrate, and added metal in the calculation (see Materials and Methods, eq 3). The resulting calculated rescue is thus specific to the double sulfur substitution only. Such a specific double sulfur substitution-dependent rescue links C208 S_P to metal M_A.

Table 3: Calculated Overall Thiophillic Metal Rescue Effects for Double Sulfur Substitution Experiments

substrate	metal	A207 R_P	A207 S_P	C208 R_P	C208 S_P [a]
3′-sulfur	1.0 mM Mn^{2+}	2.1	0.3	0.5	**0.01**
	0.5 mM Cd^{2+}	8.9	0.6	1.3	**100**
	0.5 mM Zn^{2+}	0.3	0.04	0.2	0.5
S_P sulfur	1.0 mM Mn^{2+}	1.0	0.4	1.5	**0.1**
	0.5 mM Cd^{2+}	2.0	0.8	1.7	**70**
	0.5 mM Zn^{2+}	0.8	0.2	0.2	3

[a] C208 S_P rescue with 1 mM Cd^{2+}. Rescue calculated using eq 3. Values of >1 indicate a metal-dependent rescue, while values of <1 reflect a metal-dependent inhibition. See Materials and Methods for details.

This observation leads to a strong prediction. M_A coordinates both the 3′-oxy leaving group and the *pro*-S_P oxygen of the scissile phosphate (*25*). Thio substitution of the *pro*-S_P oxygen of the scissile phosphate reduces the rate of the reaction by 10^4-fold, consistent with catalytic interactions with the *pro*-S_P oxygen (*20*). If the C208 *pro*-S_P oxygen is an active site ligand for metal M_A, then Cd^{2+} might also rescue the C208 S_P sulfur substitution when combined with a second sulfur at the S_P position of the scissile phosphate in the substrate. To test this possibility, the experiments were repeated using a substrate with an S_P phosphorothioate substitution. Again, Cd^{2+} specifically rescues activity (70-fold) when there are sulfur atoms at both the ribozyme C208 S_P position and the substrate S_P position (see Table 3) despite the fact that neither individual substitution is efficiently rescued by Cd^{2+} at this Mg^{2+} concentration (*20*, *25*). Neither Mn^{2+} nor Zn^{2+} exhibits this behavior, nor is activity rescued with Cd^{2+} for any of the other three ribozymes that were tested.

The Cd^{2+} rescue effect for both the 3′ and S_P substrates was followed as a function of concentration, although the interpretation is complicated because Cd^{2+} concentrations of >500 μM start to inhibit the reaction (see panels a and b of Figure 4). Significant rescue of activity was seen with concentrations of Cd^{2+} as low as 10 μM in the context of the 3′-thiolate substrate. At 50 μM Cd^{2+}, the rescue was complete, in that the cleavage rate of the 3′-thiolate substrate was the same for both the C208 S_P and wild-type ribozymes. The rescue effect with the S_P substrate was also significant, but not as strong as for the 3′-thiolate reaction. With the S_P substrate, the C208 S_P ribozyme rate only reached $\sim^1/_3$ of that of the wild-type ribozyme, and then only at 1 mM Cd^{2+}. Because the *pro*-S_P and 3′-oxygens in the substrate are both ligands for metal ion "A", which stabilizes the 3′-leaving group in the transition state, this localizes M_A to a binding pocket in the ribozyme that includes residue C208.

DISCUSSION

Active Site Metal Ion Coordination. Extensive biochemical research has provided a fairly complete picture of the constellation of ions contributing to the transition state in the *Tetrahymena* ribozyme cleavage reaction (*19*−*21*, *23*−

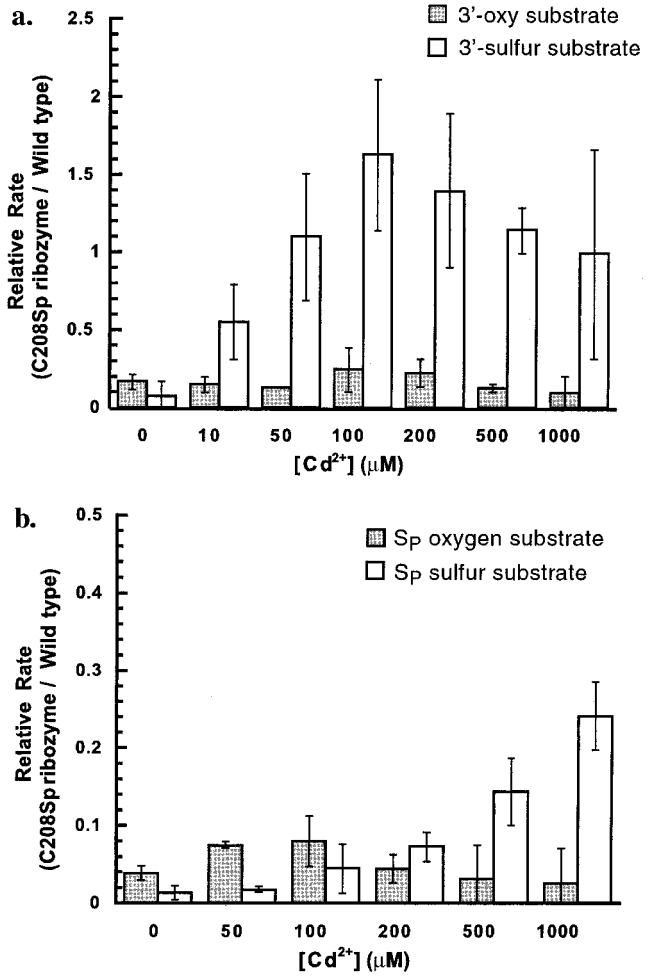

FIGURE 4: Normalized C208 S_P ribozyme rate constants as a function of Cd^{2+} concentration. (a) Plot of normalized C208 S_P ribozyme rate constants for cleavage of the 3′-oxy substrate (gray bars) and the 3′-sulfur substrate (white bars) as a function of the concentration of added Cd^{2+}. The C208 S_P sulfur substitution shows a specific and substantial rescue with Cd^{2+}, but only when the reaction involves the 3′-sulfur substrate. Experiments were carried out in a mixture of Mg^{2+} and Cd^{2+}, while maintaining a total divalent concentration of 10 mM. Data are the average of at least three independent measurements. Error bars correspond to the standard deviation from the mean. (b) Plot of the normalized C208 S_P ribozyme rate for cleavage of the S_P oxygen substrate (gray bars) and the S_P sulfur substrate (white bars) as a function of the concentration of added Cd^{2+}. The C208 S_P sulfur substitution shows a partial, but specific, rescue with Cd^{2+}, but only when the reaction involves the S_P sulfur substrate. Data are the average of at least three independent measurements. Error bars correspond to the standard deviation from the mean.

25). However, the nature of the metal interactions with the ribozyme active site has been unclear. These thiophilic metal ion rescue experiments of a double sulfur substitution define one ligand for the 3′-leaving group stabilizing metal (M_A) within the ribozyme. These data link the *pro*-S_P oxygen at residue C208 in the *Tetrahymena* ribozyme to both the 3′-oxygen and the *pro*-S_P oxygen in the ribozyme's oligonucleotide substrate (see Figure 5), two functional groups that were previously assigned to coordinate metal M_A in the transition state. While there are likely to be several such interactions with the three catalytic metal ions located in the ribozyme active site, this constitutes the first group I ribozyme ligand assigned to a specific metal ion.

Ten phosphate oxygen atoms appear to be roughly in the proximity of the substrate 3′-leaving group oxygen in the biochemically derived model for the ribozyme core (*32*, *33*). We made R_P and S_P phosphorothioate substitutions at these positions (A207, C208, A304, and U305) and at another nearby phosphate (A306). Heretofore, phosphorothioates have been incorporated into *Tetrahymena* ribozymes by T7 transcription, which only allows investigation of R_P phosphorothioates. Thus, the experiments described here allow S_P isomers at these locations to be examined for the first time. Ribozyme rates of cleavage were significantly reduced (>25-fold) for only four sulfur substitutions: A207 S_P, C208 S_P, and both substitutions at A306. As mentioned, C208 S_P is linked to M_A. In contrast, neither of the A306 substitutions, nor the A207 S_P substitution, exhibited significant rescue with any of the thiophilic metals.

Historically, rescue of activity in the presence of 1 or 2 mM Mn^{2+} has been interpreted as evidence for direct inner sphere coordination of the phosphate oxygen to a Mg^{2+} ion (*27*). Recently, however, it has been demonstrated that thiophilic metal ion rescue effects are not quite so simple to interpret. Mn^{2+} rescue can correlate with either inner sphere or outer sphere coordination to a Mg^{2+} ion, and quite often metal ligands fail to rescue with Mn^{2+}, particularly those that are tightly packed (*28*). Thus, the fact that A306 and A207 S_P substitutions cannot be rescued by metal does not necessarily mean that they do not bind a catalytic metal [although it should be pointed out that occasionally, a sulfur substitution can be structurally destabilizing, in and of itself (*45*)]. As a result, these data do not address whether the *pro*-S_P phosphate oxygen of C208 coordinates M_A directly or indirectly through a water molecule. The observation that the effects are in the range of 50-fold rather than 1000-fold might be suggestive of indirect coordination. Somewhat surprisingly, none of the phosphorothioate substitutions that were tested exhibited effects in the range of 1000-fold as might be expected for complete loss of a directly coordinated catalytic metal ion. One interpretation is that catalytic metal binding within the ribozyme active site is somewhat redundant, perhaps due to the presence of multiple ligands. In contrast, the important interactions with the substrate are uniquely important, giving rise to the larger inhibitory effects created by sulfur substitution at the 3′ or S_P positions within a substrate oligonucleotide.

In the active site scheme shown in Figure 5b, the substitutions in the J8/7 strand appear further away from M_A than the *pro*-S_P oxygen of C208, but the 2′-OH of G303 and the *pro*-S_P oxygen of U305 are in the proximity of M_A and may also be part of the metal's binding site (though caution must be taken given the low-resolution nature of the model). Substitution of a 2′-deoxy at G303 did interfere with binding and the rate of cleavage (data not shown), but obviously, this substitution cannot be rescued with a thiophilic metal, which makes it difficult to determine if the effect is due to metal ion binding or some other cause. Incorporation of a phosphorothioate at U305 S_P also reduced ribozyme activity somewhat. Because the effect was modest, we did not test it for a double sulfur substitution metal specificity switch.

Comparison of Interference and Site Specific Substitution Data. It is interesting to compare these results to previous interference data reported for the five R_P phosphorothioate-substituted ribozymes. The interference values for these

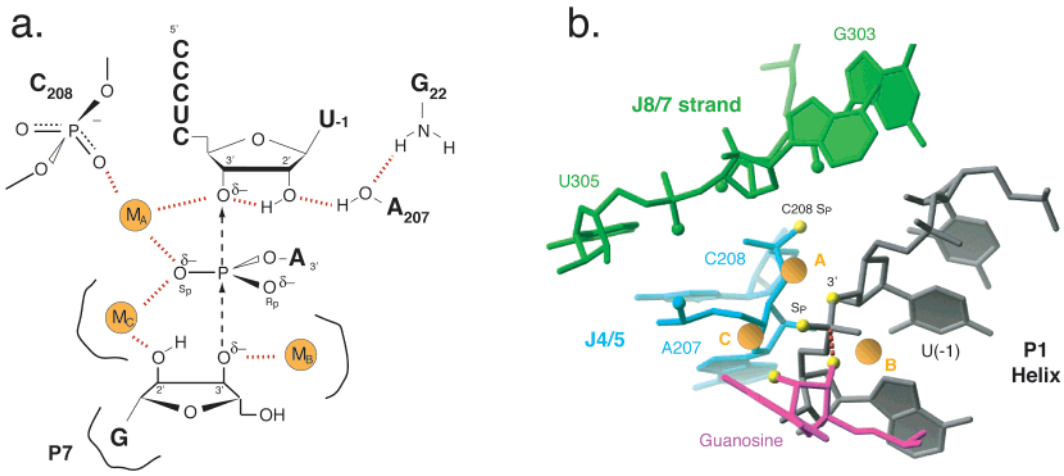

FIGURE 5: Model of the binding site for the divalent metal that stabilizes the 3′-oxygen leaving group in the *Tetrahymena* ribozyme cleavage reaction. (a) Two-dimensional scheme for the transition state in which the incoming guanosine is in the process of displacing the 5′-portion of the substrate oligonucleotide. Divalent metals are shown in gold, and red dashed lines show the network of interactions that stabilize the nucleophile and leaving group. Evidence suggests the presence of three divalent metal ions which interact with the substrate during cleavage: metal A, which interacts with the 3′-oxygen leaving group and with the S_P oxygen on the scissile phosphate (*19*, *20*); metal B, which interacts with the 3′-oxygen nucleophile on the guanosine (*21*); and metal C, which is proposed to interact with the S_P oxygen on the scissile phosphate and the 2′-OH on the guanosine (*23*, *24*). In addition, the results reported here demonstrate the existence of an interaction between the S_P oxygen of C208 and the metal which interacts with the 3′-oxygen leaving group. This is shown as a direct coordination, but the data would also be consistent with a water-mediated interaction. (b) Three-dimensional model of the *Tetrahymena* active site, with the incoming guanosine (magenta) positioned for attack at the scissile phosphate. The P1 helix substrate strand is colored gray; A207 and C208 in J4/5 are colored cyan, and residues G303, A304, and U305 in the J8/7 strand are colored green. Nearby oxygens that are potential ligands for the divalent metals are enlarged for clarity. Colored in yellow are those oxygens known to interact with the divalent metals in the active site. Substrate S_P and 3′-oxygens are labeled, as is the S_P oxygen of C208. Metals in the active site are colored orange and labeled according to the method used for panel a. See the text for discussion.

phosphorothioates are as follows: 1 for A207 R_P, 6 for C208 R_P, 2.5 for A304 R_P, 6 for U305 R_P, and 6 for A306 R_P, where a value of 1 represents no effect, values of 2−4 are considered moderate effects, and large effects are assigned a maximum value of 6 (*44*). These data correlate very nicely with the magnitude of the effects observed upon single-site substitution. As expected, strong effects for substrate binding or catalysis were observed at C208 R_P, U305 R_P, and A306 R_P, and little effect was observed at A207 R_P. A304 R_P exhibited a 2-fold effect on substrate affinity that reflects the modest observed interference value of 2.5. Reduced substrate affinity could be particularly important within the competitive environment of the group I intron interference assay. Obviously, interference data could not be obtained for any of the S_P phosphorothioate substitutions.

Comparison to Previous Active Site Metal Ion Models. Previous work has modeled the catalytic metal ions within the group I intron active site. Streicher et al. (*46*) positioned two active site metals within the Michel−Westhof group I intron model (*47*, *48*), based upon the existence of Ca^{2+}-, Sr^{2+}-, Mn^{2+}-, and Pb^{2+}-induced cleavage in the *td* group I intron at nucleotide U305 in the J8/7 strand (*Tetrahymena* numbering) and the fact that Mg^{2+} could compete away such cleavage. In their model, M_A (depicted as Mg^{2+} B in Figure 8 of ref *46*) was proposed to interact with the *pro*-R_P phosphate oxygens of U305 and A308 in J8/7. Metal M_B, the metal that activates the 3′-OH nucleophile of guanosine (depicted as Mg^{2+} A in Figure 8 of ref *46*), was predicted to lie on the same side of the substrate strand as M_A and to coordinate the *pro*-R_P phosphate oxygen of A306 and N3 of A263. Although specific proposals were made, no experimental evidence was used to directly link any of these functional groups to a particular metal ion.

Consistent with the cleavage results, it is quite likely that these residues are close to or within the active site, but the details of this earlier proposal are likely to require some revision. Recent work has also shown that M_B must lie on the opposite side of the substrate strand from M_A and that there is a third metal, M_C, in the active site that must also be accommodated (*25*, *49*). The work presented here provides evidence that M_A is coordinated to C208, but it provides no compelling support for a catalytic contribution by the *pro*-R_P oxygen of U305 as suggested in the model of Streicher et al. A308 was not tested in this study, though it did display a strong phosphorothioate effect in an interference analysis of a bacterial intron (*44*). The strong phosphorothioate effects observed at A306 are consistent with the proposed coordination to metal M_B, though the lack of any thiophilic metal rescue leaves the data inconclusive.

In conclusion, our results provide biochemical evidence that links the *pro*-S_P oxygen of C208 with the 3′-leaving group oxygen and the *pro*-S_P oxygen within the substrate oligonucleotide. Thus, one of the catalytic metals that stabilize the group I intron transition state has, for the first time, been localized within the ribozyme active site. It is reasonable to expect that other RNA functional groups serve as ligands for active site metals, though no more specific assignments can be made from the current data.

ACKNOWLEDGMENT

We thank Lara Szewczak for helpful comments on the manuscript, Rebecca Charnas for construction of the plasmid pUCP9, and Aiichiro Yoshida and Cecilia Cortez for assistance with preparation of the 3′-S substrate.

REFERENCES

1. Gesteland, R. F., Cech, T., and Atkins, J. F. (1999) *The RNA World*, 2nd ed., Cold Spring Harbor Laboratory Press, Plainview, NY.
2. Wimberly, B. T., Brodersen, D. E., Clemons, W. M., Jr., Morgan-Warren, R. J., Carter, A. P., Vonrhein, C., Hartsch, T., and Ramakrishnan, V. (2000) *Nature 407*, 327−339.
3. Ban, N., Nissen, P., Hansen, J., Moore, P. B., and Steitz, T. A. (2000) *Science 289*, 905−920.
4. Nissen, P., Hansen, J., Ban, N., Moore, P. B., and Steitz, T. A. (2000) *Science 289*, 920−930.
5. Nakano, S., Chadalavada, D. M., and Bevilacqua, P. C. (2000) *Science 287*, 1493−1497.
6. Perrotta, A. T., Shih, I., and Been, M. D. (1999) *Science 286*, 123−126.
7. Rupert, P. B., and Ferre-D'Amare, A. R. (2001) *Nature 410*, 780−786.
8. Ryder, S. P., Oyelere, A. K., Padilla, J. L., Klostermeier, D., Millar, D. P., and Strobel, S. A. (2001) *RNA* (in press).
9. Muth, G. W., Ortoleva-Donnelly, L., and Strobel, S. A. (2000) *Science 289*, 947−950.
10. Golden, B. L., and Cech, T. R. (1999) in *The RNA World* (Gesteland, R. F., Cech, T. R., and Atkins, J. F., Eds.) 2nd ed., Cold Spring Harbor Press, Plainview, NY.
11. Sontheimer, E. J., Sun, S., and Piccirilli, J. A. (1997) *Nature 388*, 801−805.
12. Steitz, T. A., and Steitz, J. A. (1993) *Proc. Natl. Acad. Sci. U.S.A. 90*, 6498−6502.
13. Smith, D., and Pace, N. R. (1993) *Biochemistry 32*, 5273−5281.
14. Yean, S. L., Wuenschell, G., Termini, J., and Lin, R. J. (2000) *Nature 408*, 881−884.
15. Gordon, P. M., Sontheimer, E. J., and Piccirilli, J. A. (2000) *Biochemistry 39*, 12939−12952.
16. Christian, E. L., Kaye, N. M., and Harris, M. E. (2000) *RNA 6*, 511−519.
17. Gordon, P. M., and Piccirilli, J. A. (2001) *Nat. Struct. Biol. 8*, 893−898.
18. Grosshans, C. A., and Cech, T. R. (1989) *Biochemistry 28*, 6888−6894.
19. Piccirilli, J. A., Vyle, J. S., Caruthers, M. H., and Cech, T. R. (1993) *Nature 361*, 85−88.
20. Yoshida, A., Sun, S., and Piccirilli, J. A. (1999) *Nat. Struct. Biol. 6*, 318−321.
21. Weinstein, L. B., Jones, B. C. N. M., Cosstick, R., and Cech, T. R. (1997) *Nature 388*, 805−808.
22. Pecoraro, V. L., Hermes, J. D., and Cleland, W. W. (1984) *Biochemistry 23*, 5262−5271.
23. Sjogren, A. S., Pettersson, E., Sjoberg, B. M., and Stromberg, R. (1997) *Nucleic Acids Res. 25*, 648−653.
24. Shan, S., Yoshida, A., Sun, S., Piccirilli, J. A., and Herschlag, D. (1999) *Proc. Natl. Acad. Sci. U.S.A. 96*, 12299−12304.
25. Shan, S., Kravchuk, A. V., Piccirilli, J. A., and Herschlag, D. (2001) *Biochemistry 40*, 5161−5171.
26. Christian, E. L., and Yarus, M. (1992) *J. Mol. Biol. 228*, 743−758.
27. Christian, E. L., and Yarus, M. (1993) *Biochemistry 32*, 4475−4480.
28. Basu, S., and Strobel, S. A. (1999) *RNA 5*, 1399−1407.
29. Ortoleva-Donnelly, L., Szewczak, A. A., Gutell, R. R., and Strobel, S. A. (1998) *RNA 4*, 498−519.
30. Strobel, S. A., and Shetty, K. (1997) *Proc. Natl. Acad. Sci. U.S.A. 94*, 2903−2908.
31. Strobel, S. A., Ortoleva-Donnelly, L., Ryder, S. P., Cate, J. H., and Moncoeur, E. (1998) *Nat. Struct. Biol. 5*, 60−66.
32. Szewczak, A. A., Ortoleva-Donnelly, L., Ryder, S., and Strobel, S. A. (1998) *Nat. Struct. Biol. 5*, 1037−1042.
33. Szewczak, A. A., Ortoleva-Donnelly, L., Zivarts, M. V., Oyelere, A. K., Kazantsev, A. V., and Strobel, S. A. (1999) *Proc. Natl. Acad. Sci. U.S.A. 96*, 11183−11188.
34. Strobel, S. A., and Ortoleva-Donnelly, L. (1999) *Chem. Biol. 6*, 153−165.
35. Nakamura, T. M., Wang, Y. H., Zaug, A. J., Griffith, J. D., and Cech, T. R. (1995) *EMBO J. 14*, 4849−4859.
36. Doudna, J. A., and Szostak, J. W. (1989) *Mol. Cell. Biol. 9*, 5480−5483.
37. Scaringe, S. A., Wincott, F. E., and Caruthers, M. H. (1998) *J. Am. Chem. Soc. 120*, 11820−11821.
38. Burgers, P. M., and Eckstein, F. (1978) *Proc. Natl. Acad. Sci. U.S.A. 75*, 4798−4800.
39. Herschlag, D., Piccirilli, J. A., and Cech, T. R. (1991) *Biochemistry 30*, 4844−4854.
40. Sun, S., Yoshida, A., and Piccirilli, J. A. (1997) *RNA 3*, 1352−1363.
41. Moore, M. J., and Sharp, P. A. (1992) *Science 256*, 992−997.
42. Pyle, A. M., McSwiggen, J. A., and Cech, T. R. (1990) *Proc. Natl. Acad. Sci. U.S.A. 87*, 8187−8191.
43. Herschlag, D., and Cech, T. R. (1990) *Biochemistry 29*, 10159−10171.
44. Strauss-Soukup, J. K., and Strobel, S. A. (2000) *J. Mol. Biol. 302*, 339−358.
45. Smith, J. S., and Nikonowicz, E. P. (2000) *Biochemistry 39*, 5642−5652.
46. Streicher, B., Westhof, E., and Schroeder, R. (1996) *EMBO J. 15*, 2556−2564.
47. Lehnert, V., Jaeger, L., Michel, F., and Westhof, E. (1996) *Chem. Biol. 3*, 993−1009.
48. Michel, F., and Westhof, E. (1990) *J. Mol. Biol. 216*, 585−610.
49. Yoshida, A., Shan, S., Herschlag, D., and Piccirilli, J. A. (2000) *Chem. Biol. 7*, 85−96.
50. Cech, T. R., Damberger, S. H., and Gutell, R. R. (1994) *Nat. Struct. Biol. 1*, 273−280.

BI011973U